



Research Article

DEVICE DESIGN OF 3-NM NODE-COMPLEMENTARY-FIELD EFFECT TRANSISTOR (CFET)Dalwadi Nirmalkumar Rameshbhai¹, Anshuj Jain² and Laxmi Singh³

Department of Electronics and communication Engineering, Rabindranath Tagore University Raisen ,India

ARTICLE INFO

Article History:Received 11th April, 2024Received in revised form 26th April, 2024Accepted 18th May, 2024Published online 28th May, 2024**Key words:**

3-nm technology node, Nanosheet FET (NSHFET), Complementary FET, TCAD

ABSTRACT

With a common gate, this CFET vertically stacks n-type and p-type nanosheet MOSFETs. Here, the ideal CFET device dimensions are examined in order to improve the electrical properties and inverter performance. Performance is examined for a number of CFET vertical dimension factors, encompassing how many stacked channels there are, the vertical distance (D_{nsh}) between nanosheet channels, the distance (D_{n/p}) between MOS separations, and the channel thickness (T_{nsh}). The findings indicate that, in contrast to typical CMOS, CFETs may efficiently increase inverter performance without experiencing significant deterioration by reducing their D_{nsh} and D_{n/p}, even though doing so forces a harsh trade-off between various parameters due to other dimensional factors. Due to electrical coupling, the decrease in D_{nsh} and D_{n/p} in the case of electrical characteristics marginally but significantly raises T_{max} and R_{th}. Thus, a key technique for the creation of sub-3-nm CFETs will be the lowering of D_{nsh} and D_{n/p}.

Copyright© The author(s) 2024. This is an open access article distributed under the Creative Commons Attribution License, which permits unrestricted use, distribution, and reproduction in any medium, provided the original work is properly cited.

INTRODUCTION

Conventional FinFETs, which have recently been scaled down to 5-nm nodes, have almost reached physical limits in reducing fin thickness [1]. Thus, to improve gate controllability, nanosheet FETs (NSHFETs) with gate-all around (GAA) structures have been actively developed for sub-3-nm nodes [1]–[3]. However, they will continue to face these down-scaling limitations in the future. Therefore, to reduce the number of tracks and layout area to reduce the device footprint, the International Roadmap for Devices and Systems (IRDS) expects that a 3-dimensional structure which stacks multiple NSHFETs vertically can be a strong candidate for future technology nodes [4]–[11]. Thus, one of the most promising devices with a 3-dimensional structure, (CFET), which stacks n-NSHFET and p-NSHFET vertically with a shared gate for CMOS inverter operation in one device, has recently been suggested by Intel, Applied Materials, IMEC, and NARLab [4]–[9]. In addition, in a recent study on CFET, it was demonstrated that CFET with NSHFET shows better inverter performance than CFET with FinFET [8]. Recently, NSHFET have been replacing FinFETs for logic devices because of higher inverter operation frequency (f). This is owed to the lower effective resistance (R_{eff}) of NSHFETs due to better current drivability and gate controllability in the same footprint [1]. However, the large effective capacitance (C_{eff}) of NSHFETs disturbs additional improvement of f or power-product delay (PDP). Therefore, a decrement of C_{eff} is an important factor for improving inverter performances. Furthermore, the CFET, which stacks vertically stacked NSHFETs also faces performance degradation by high C_{eff}

because of the additional height of metal via of the vertically stacked structure. Recent studies demonstrated that CFET shows the possibility for better C_{eff} compared with conventional CMOS with NSHFETs because of fringe electric field overlap triggered by the reduced distance between nMOS and pMOS with the vertically stacked structure [4], [10]. In addition, recent fabrication processes demonstrated by Intel reduced number of metal via by connecting the drain of the nMOS and pMOS with one piece of metal via. This could additionally decrease C_{eff}.

However, CFET has a much higher height of metal via compared with conventional CMOS because of the stacked structure of the nMOS and pMOS. Therefore, there is still a risk of the degradation of C_{eff}, and the careful design of CFET is required. Therefore, analyzing C_{eff} and R_{eff} of the CFET by varying dimensions is required to evaluate f and PDP [3]. In addition, it has been reported that multi-gate transistors such as NSHFETs are vulnerable to the self-heating effect (SHE) because of their confined geometry, which triggers thermal reliability issues [12]–[19]. In particular, it is expected that the high height of CFET makes it difficult for heat to dissipate to the thermal ground. Thus, finding a way to alleviate the SHE in CFET by stacking nNSHFETs and pNSHFETs is important. However, there has been no qualitative analysis of the optimal design of CFETs based on both thermal characteristics and CMOS inverter performances for different dimensions.

For the first time, the device design guideline of the 3-nm node CFET is investigated from the perspective of thermal

*Corresponding author: Dalwadi Nirmalkumar Rameshbhai

Department of Electronics and communication Engineering, Rabindranath Tagore University Raisen ,India

characteristics and CMOS inverter accomplishment with carefully calibrated 3-D TCAD. First, the CMOS inverter performances of C_{eff} , R_{eff} , f , and PDP in the 3-nm node CFET are analyzed by varying the dimensions of the number of stacked channels (NnMOS, NpMOS), distance between the nanosheets (D_{nsh}), n/pMOS separation distances ($D_{n/p}$), nanosheet channel thickness (T_{nsh}), and nanosheet width (W_{nsh}). Moreover, the maximum lattice temperature (T_{max}) and thermal resistance (R_{th}) is evaluated in terms of different dimensions. Finally, the impact of the device design on the inverter performance and thermal characteristics is analyzed from the perspective of down-scaling.

MODELING METHODOLOGY

The 3-nm node CFET was designed for the front-end-of line (FEOL) based on the high-performance specification. The structure of CFET was based on the experimental reference of Intel [9]. Fig. 1 shows the schematics of the 3-nm node CFET. Fig. 2 shows a 3-D bird's eye view of the CFET. Fig. 3, 4, 5, and 6 show the cross-sectional view of the 3-nm node CFET and schematics with structural parameters.

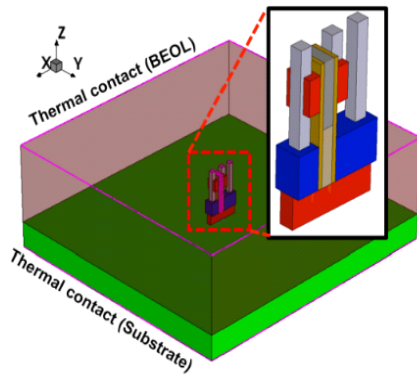


Fig. 1 3-nm node CFET

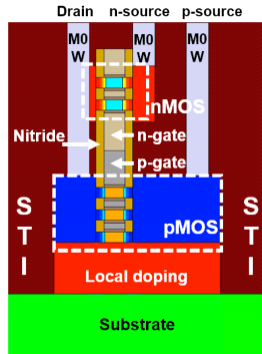


Fig. 2 CFET's cross-sectional view

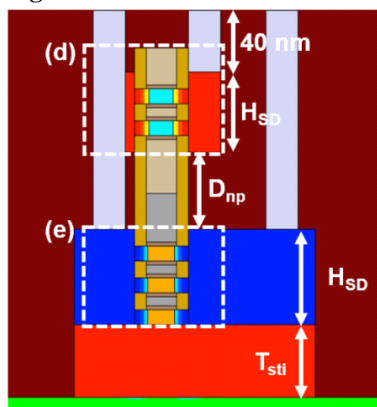


Fig. 3 Parameters of CFET in cross-sectional view

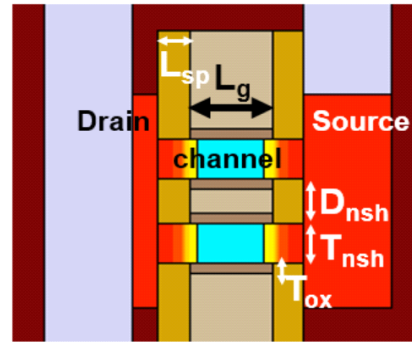


Fig. 4 CFET in cross-sectional view nMOS

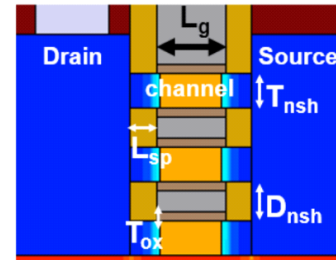


Fig. 5 parameters of CFET in cross-sectional view nMOS Table 1 shows the structural parameters used in TCAD, and the reference values of each parameter are underlined.

Table 1 Structural parameters used for 3-nm complementary FET and reference values (underlined).

Quantity	Value	Description
L_{gate}	16 nm	Physical gate length
T_{oxide}	2 nm	Gate oxide thickness
N_{nMOS}	1, <u>2</u> , 3, 4	Number of stacked n-channel
N_{pMOS}	2, <u>3</u> , 4, 5	Number of stacked p-channel
W_{nsh}	15, 17.5, <u>20</u> , 22.5, 25 nm	Nanosheet channel width
T_{nsh}	6, 7, <u>8</u> , 9, 10 nm	Nanosheet channel thickness
D_{nsh}	7, 8, <u>9</u> , 10, 11 nm	Distance between nanosheets
$D_{n/p}$	20, 30, 40, <u>50</u> , 60, 70 nm	n/pMOS separation
$L_{S/D}$	10 nm	Source/drain (S/D) length
L_{spacer}	6 nm	Spacer length
$N_{it,nMOS}$	$5 \times 10^{12} \text{ cm}^{-3}$ (Acceptor)	Interface trap conc. of nMOS
$N_{it,pMOS}$	$1 \times 10^{12} \text{ cm}^{-3}$ (Donor)	Interface trap conc. of pMOS
Quantity	Doping concentration	Description
$N_{S/D} \text{ (nMOS)}$	$1 \times 10^{21} \text{ cm}^{-3}$	S/D doping concentration
$N_{S/D} \text{ (pMOS)}$	$1 \times 10^{21} \text{ cm}^{-3}$	S/D doping concentration
$N_{sub} \text{ (nMOS)}$	$1 \times 10^{18} \text{ cm}^{-3}$	Substrate doping concentration
$N_{sub} \text{ (pMOS)}$	$1 \times 10^{19} \text{ cm}^{-3}$	Substrate doping concentration
N_{Local}	$1 \times 10^{19} \text{ cm}^{-3}$	Local doping concentration

For CFET, nMOS-on-pMOS structure is assumed based on [9]. The physical gate length (L_g) was set as 16 nm. For the gate oxide, 2-nm thick HfO_2 was used. In addition, gate metal, which has a work function of 4.54 eV and 4.8 eV, is used for nMOS and pMOS of CFET respectively.

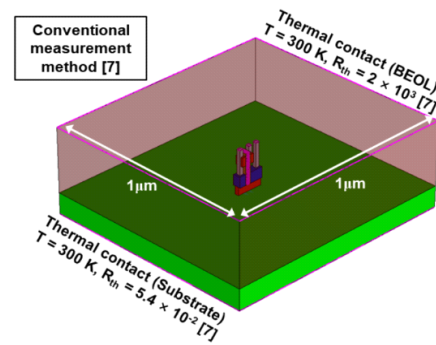


Fig.6 The 3-nm node CFET with boundary conditions.

Fig. 6 shows schematics of the thermal parameters used in TCAD. Thermal modeling is based on the simulation setup of the conventional model suggested by [12]–[19]. As shown in Fig. 6, the CFET locates on a wide silicon substrate and is surrounded by SiO₂. Boundaries are then set on the top and bottom surfaces for realistic heat dissipation modeling [12].

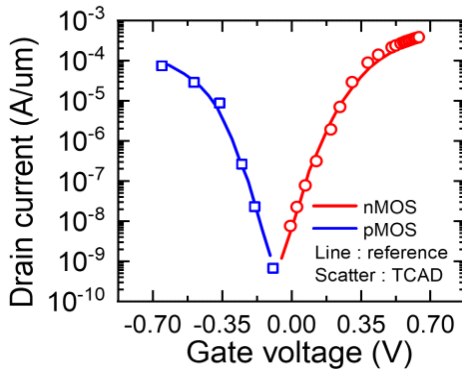


Fig.8 Calibrated transfer characteristics of CFET.

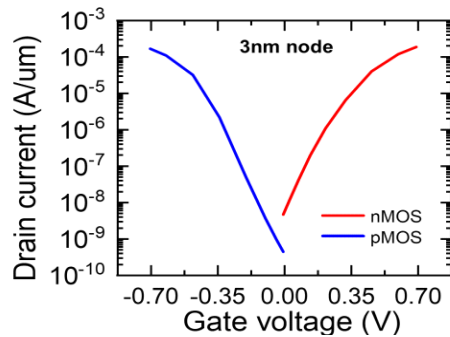


Fig.9 Transfer characteristic of CFET, for the 3-nm

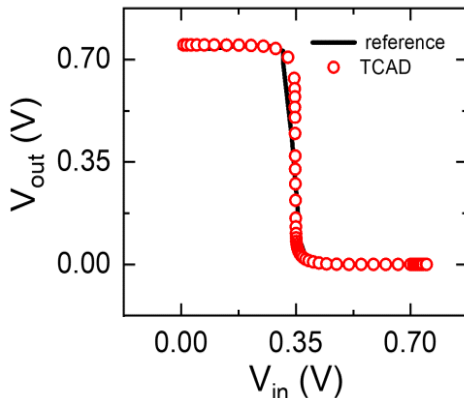


Fig.10 VTC of CFET

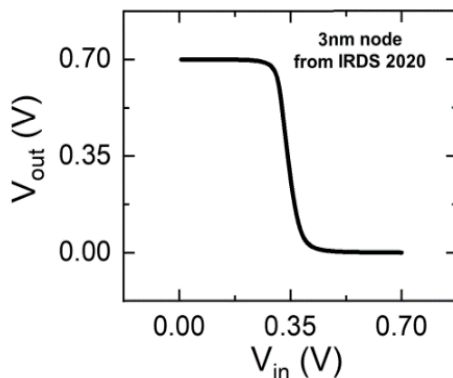


Fig.11 VTC of CFET for the 3-nm node

Fig. 8 shows the method of calibration of the TCAD to reference for realistic simulation. The calibration of TCAD is

performed for the transfer characteristic and voltage transfer characteristic (VTC) of CFET (Fig. 8 and 10) from the experimental reference with a gate length of 75 nm [7].

This is the only fabricated CFET with vertically stacked NSHFETs that can operate as inverters with a high on state current and low SS. Then, a 3-nm node CFET is designed using the IRDS specifications, as shown in Table 1, and the DC performances and inverter performances.

For device physics, models of density gradient quantum correction and inversion accumulation mobility are used to consider quantum confinement in Nano scale devices.

In addition, bandgap narrowing, electric-field-dependent mobility, doping-dependent mobility, high field saturation, Shockley-Read-Hall doping dependence and band-to-band tunneling (Hurkx) were used. Parameters for respective physics are used from default value provided TCAD. The model was also applied to simulate realistic carrier transportation with the parameters listed in Table 2 [12]–[19].

The transient response of the 3-nm node CFET. The transient response of the 3-nm node CFET is calculated by “mixed-mode” of TCAD. The power supply voltage (V_{dd}) is set to 0.6 V. For the transient response, the inverter performance is calculated based on the fan-out of the 3 (FO3) logic inverter circuit. [20], [21].

Here, C_{eff} is calculated from the general equation

$C_{eff} = \text{total gate capacitance}(C_{gg}) + \text{total drain capacitance}(C_{dd}) + 3 (\text{number of fanout devices}) \times \text{fan-out capacitance}(C_{fo})$ [20], [21].

C_{fo} is assumed to be the same as C_{gg}

Therefore

$$C_{eff} = 4 \times C_{gg} + C_{dd}.$$

C_{gg} and C_{dd} are extracted from a single CFET device.

Here, C_{gg} includes the gate-to-drain capacitance (C_{gd}), gate-to-source capacitance of nMOS (C_{gsn}), and gate to-source capacitance of pMOS (C_{gsp}). For the performance parameters, f is extracted using the equation shown in Fig.13.

Power is calculated using $C_{eff} \times f \times V_{dd}^2$,

PDP is calculated as power/f,

Reff is calculated as $1 / (C_{eff} \times f)$ [20], [21].

RESULTS AND DISCUSSION

To investigate the inverter performance characteristics, f, power, C_{eff}, and Reff of the 3-nm node CFET were compared for different structures and dimensions. f, PDP, C_{eff}, and Reff for different numbers of stacked channels of nMOS and pMOS (N_nMOS, N_pMOS) are compared. For N_nMOS and N_pMOS, N_nMOS/N_pMOS of 1/2, 2/3, 3/4, and 4/5 were used to compare inverter performances of the 3-nm node CFET for different N_nMOS and N_pMOS. For each device with N_nMOS/N_pMOS, the transfer characteristics of the nMOS and pMOS were calibrated to obtain the same VTC characteristics. N_pMOS was chosen for a higher number than N_nMOS to match the drain current, because the mobility of nMOS is much lower than that of pMOS. where f is calculated as $1 / (Reff \times C_{eff})$. The increment of N_nMOS and N_pMOS induces a higher drive current (I_{drive}) because of the large effective width and reduces Reff; however, C_{eff} increases as the gate area and height of the metal via increase. The device with N_nMOS of 2 and N_pMOS of 3 shows the highest f. PDP is calculated as $C_{eff} \times V_{dd}^2$ in general; therefore, PDP is

proportional to C_{eff} [20], [21]. Thus, the increment in f in nMOS and pMOS triggers an increment in C_{eff} , so PDP increases. C_{eff} changes linearly by different dimensions, but R_{th} changes non-linearly. The reason of R_{th} 's non-linearity is the impact of physics. Increment of current with increment of dimensions increases device temperature. The increased temperature degrades current and increases R_{th} . In f , PDP, C_{eff} , and R_{th} are compared for different values of D_{nsh} , $D_{n/p}$, T_{nsh} , and W_{nsh} . For D_{nsh} and $D_{n/p}$, ranges of 7–11 nm and 20–70 nm were used, respectively. In addition, W_{nsh} and T_{nsh} , ranging from 15 to 25 nm and 6 to 10 nm, respectively, were used. For D_{nsh} and $D_{n/p}$ in increase in D_{nsh} and $D_{n/p}$ can reduce f and increase PDP. The changes in D_{nsh} and $D_{n/p}$ rarely cause a change in R_{th} as the effective width is constant and I_{drive} does not change. Therefore, C_{eff} dominantly determines f for the changes in D_{nsh} and $D_{n/p}$. Here, the reduction of both D_{nsh} and $D_{n/p}$ triggers a low C_{eff} .

This is because the gate fringe electric field overlap is triggered between nMOS and pMOS of the CFET with a vertically stacked structure [4], [10]. In addition, the reduced height of the metal via decreases C_{eff} [10]. Thus, f increases with a reduction in D_{nsh} and $D_{n/p}$. Since PDP is proportional to C_{eff} , the reduction in D_{nsh} and $D_{n/p}$ can decrease PDP with lower C_{eff} . The device with the optimum values for T_{nsh} of 9 nm and W_{nsh} of 21 nm is required for the highest f . Thus, a higher effective width decreases R_{th} , and a larger gate area increases C_{eff} with increasing T_{nsh} and W_{nsh} . In addition, because of the increase in C_{eff} , PDP increases with increasing T_{nsh} and W_{nsh} .

CONCLUSION

3-D TCAD calibration, the inverter performance and thermal properties of a 3-nm node CFET with varying dimensions were examined for the first time. Furthermore, recommendations for CFET device design were made in order to improve the inverter's performance and thermal properties. First, inverter performances by different nMOS, pMOS, D_{nsh} , $D_{n/p}$, T_{nsh} , and W_{nsh} were investigated. For nMOS and pMOS, with a reduction in the above parameters, C_{eff} decreases because the gate area decreases and the height of the metal via is reduced. However, R_{th} increases with a decrease in the effective width. Therefore, an optimum nMOS/pMOS ratio of 2/3 is required for the highest f as a trade-off between C_{eff} and R_{th} . For D_{nsh} and $D_{n/p}$, their reduction decreases the height of the metal gate and source/drain metal via, thereby reducing C_{eff} without changing R_{th} . Thus, the reduction of D_{nsh} and $D_{n/p}$ can increase f and decrease PDP. Subsequently, the thermal characteristics by different nMOS, pMOS, D_{nsh} , $D_{n/p}$, T_{nsh} , and W_{nsh} were investigated. For the different nMOS and pMOS, their reduction decreases the gate area and disturbs the heat dissipation from the devices to the thermal ground, thereby increasing R_{th} . In the case of D_{nsh} and $D_{n/p}$, their reduction induces a higher R_{th} because of severe thermal coupling, but the change in R_{th} is negligible. Considering both inverter accomplishment and thermal characteristics from the perspective of down-scaling, it is notable that the reduction in D_{nsh} and $D_{n/p}$ of CFET can improve both f and PDP without severe degradation. This is different from the other dimension parameters; results demonstrate a significant trade-off between thermal parameters and inverter performance. This study can provide crucial insights into the device design of CFET for a sub-3-nm node.

Acknowledgements

The authors would like to thank Dr. Laxmi Singh for their helpful support.

References

1. P. Weckx et al., "Novel forksheet device architecture as ultimate logic scaling device towards 2 nm," in IEDM Tech. Dig., Dec. 2019, pp. 871–874, doi: 10.1109/IEDM19573.2019.8993635.
2. J. Ryckaert et al., "The complementary FET (CFET) for CMOS scaling beyond N3," Proc. IEEE Symp. VLSI Technol., Jun. 2018, pp. 141–142, doi: 10.1109/VLSIT.2018.8510618.
3. S.-W. Chang et al., "First demonstration of CMOS inverter and 6T-SRAM based on GAA CFETs structure for 3D-IC applications," in Proc. IEEE Int. Electron Devices Meeting (IEDM), 2019, pp. 11.7.1–11.7.4, doi: 10.1109/IEDM19573.2019.8993525.
4. S. Subramanian et al., "First monolithic integration of 3D complementary FET (CFET) on 300mm Wafers," in Proc. IEEE Symp. VLSI Technol., 2020, pp. 1–2, doi: 10.1109/VLSITechnology18217.2020.9265073.
5. C.-Y. Huang et al., "3-D self-aligned stacked NMOS-on-PMOS nanoribbon transistors for continued Moore's Law scaling," in Proc. IEEE Int. Electron Devices Meeting (IEDM), 2020, pp. 20.6.1–20.6.4, doi: 10.1109/IEDM13553.2020.9372066.
6. M. G. Bardon et al., "Power-performance trade-offs for lateral nanosheets on ultra-scaled standard cells," in Proc. IEEE Symp. VLSI Technol., 2018, pp. 143–144, doi: 10.1109/VLSIT.2018.8510633.
7. D. Yakimets et al., "Power aware FinFET and lateral nanosheet FET targeting for 3nm CMOS technology," in Proc. IEEE Int. Electron Devices Meeting (IEDM), 2017, pp. 20.4.1–20.4.4, doi: 10.1109/IEDM.2017.8268429.
8. P. Schuddinck et al., "Device- circuit- & block-level evaluation of CFET in a 4 track library," in Proc. Symp. VLSI Technol., Jun. 2019, pp. T204–T205, doi: 10.23919/VLSIT.2019.8776513.
9. "International Roadmap for Devices and Systems (IRDS)." 2020. [Online]. Available: <https://irds.ieee.org/editions/2020>
10. T. Cui, Q. Xie, Y. Wang, S. Nazarian, and M. Pedram, "7nm FinFET standard cell layout characterization and power density prediction in near- and super-threshold voltage regimes," in Proc. Int. Green Comput. Conf., 2014, pp. 1–7, doi: 10.1109/IGCC.2014.7039170.
11. J. M. Rabaey, A. Chandrakasan, B. Nikolic, Digital Integrated Circuits: A Design Perspective. Englewood Cliffs, NJ, USA: Prentice Hall, 1996.
12. Y. Taur and T. H. Ning. Fundamentals of Modern VLSI Devices. Cambridge, U.K.: Cambridge Univ. Press, 2009. doi: 10.1109/IEDM19574.2021.9720601.
13. J. Ryckaert et al., "The Complementary FET (CFET) for CMOS scaling beyond N3," in Proc. IEEE Symp. VLSI Technol., Jun. 2018, pp. 141–142, doi: 10.1109/VLSIT.2018.8510618.
14. C.-Y. Huang et al., "3-D self-aligned stacked NMOS-on-PMOS nanoribbon transistors for continued Moore's law scaling," in IEEE Int. Electron Devices

Meeting Tech. Dig., Dec. 2020, pp. 20.6.1–20.6.4, doi: 10.1109/IEDM13553.2020.9372066.

15. S.-W. Chang et al., “First demonstration of CMOS inverter and 6T-SRAM based on GAA CFETs structure for 3D-IC applications,” in IEEE Int. Electron Devices Meeting Tech. Dig., Dec. 2020, pp. 11.7.1–11.7.4, doi: 10.1109/IEDM19573.2019.8993525.
16. T.-Z. Hong et al., “First demonstration of heterogenous complementary FETs utilizing low-temperature (200°C) hetero-layers bonding technique (LT-HBT),” in IEEE Int. Electron Devices Tech. Dig., Dec. 2020, pp. 15.5.1–15.5.4, doi: 10.1109/IEDM13553.2020.9372001.
17. Y.-J. Lee et al., “Low-temperature microwave annealing for MOSFETs with high-k/metal gate stacks,” IEEE Electron Device Lett., vol. 34, no. 10, pp. 1286–1288, Oct. 2013, doi: 10.1109/LED.2013.2279396.
18. Sentaurus TCAD Version 2019, Synopsys, Mountain View, CA, USA, 2019.
19. R. Zhang, X. Yu, M. Takenaka, and S. Takagi, “Impact of channel orientation on electrical properties of Ge p- and n-MOSFETs with 1-nm EOT Al₂O₃/GeO_x/Ge gate-stacks fabricated by plasma postoxidation,” IEEE Trans. Electron Devices, vol. 61, no. 11, pp. 3668–3675, Nov. 2014, doi: 10.1109/TED.2014.2359678.
20. L. P. B. Lima, H. F. W. Dekkers, J. G. Lisoni, J. A. Diniz, S. Van Elshocht, and S. De Gendt, “Metal gate work function tuning by Al incorporation in TiN,” J. Appl.
21. S. Subramanian et al., “First monolithic integration of 3D complementary FET (CFET) on 300mm wafers,” in Proc. IEEE Symp. VLSI Technol., Jun. 2020, pp. 1–2, doi: 10.1109/VLSITechnology18217.2020.9265073.

Biographies of Authors



Dalwadi Nirmalkumar Rameshbhai graduated in Electronics and communication engineering from sunrise University, Rajasthan in 2016. He received the Master in Digital communication Engineering from Sunrise University, Rajasthan in 2018. He is joined the Shri.j.m.sabva institute of engineering & technology affiliated by Gujarat technological University as an Assistant professor. His current research interests include VLSI implementation with advanced nanometer cell technologies design and privacy preserving deep learning models and federated learning.



Dr. Laxmi Singh graduated from the Electronic Department of Oriental Institute of Science and Technology with honors and received the M.Tech degrees in VLSI from the RKDF Institute of Science and Technology in 2007 and 2011, respectively. Subsequently, she carried out her research from RNTU Bhopal and awarded Ph.D. in 2015. Presently, she is working as Professor in the Department of Electronics and Communication at RNTU, Bhopal. Her research area includes VLSI Design, Signal Processing and Image processing.

How to cite this article:

Dalwadi Nirmalkumar Rameshbhai, Anshuj Jain and Laxmi Singh. (2024). Device Design of 3-Nm Node-Complementary-Field Effect Transistor (CFET). *International Journal of Current Advanced Research*. 13(05), pp.3143-3147.
